2021 EAGE ANNUAL
82ND CONFERENCE & EXHIBITION
AMSTERDAM | THE NETHERLANDS

LEAST-SQUARES MULTIPLE IMAGING CONSTRAINED JOINTLY BY OBN AND TOWED-STREAMER DATA

G. Poole[1]

[1] CGG

Summary

Marine seismic surveys in shallow water regions typically suffer from acquisition striping and poor shallow resolution. Multiple imaging has been discussed in the literature for several years as a processing-based approach to this problem. We compare least-squares wave-equation multiple migration (LS-WEMM) results for towed-streamer and ocean bottom node (OBN) data sets co-located in the Central North Sea. With either data type, LS-WEMM results reduce acquisition striping and improve spatial resolution, when compared with primary imaging. Further, we observe that the towed-streamer LS-WEMM result provides better lateral resolution than the OBN LS-WEMM result, whereas the OBN LS-WEMM result provides better image illumination overall. We propose a LS-WEMM method constrained jointly by towed-streamer and OBN data, which is shown to combine the benefits offered by both data types.

Least-squares multiple imaging constrained jointly by OBN and towed-streamer data

Introduction

The use of efficient wide-tow streamer acquisition limits the availability of short-offset primary arrivals for shallow imaging. This results in strong acquisition striping and poor vertical resolution, making interpretation of the shallow section difficult. While data interpolation and regularisation can help reduce striping, the vertical resolution of the shallow section may still be problematic. Acquisition approaches to alleviate this problem include reducing the sail-line spacing, placing the sources closer to (Dhelie et al., 2020) or above (Vinje et al., 2017) the streamers, and nearfield hydrophone (NFH) imaging (Davies and Tillotson, 2019). However, these approaches come with increased acquisition cost, or incomplete coverage in the case of NFH imaging for multi-streamer surveys.

The imaging of free-surface multiples offers a data-driven alternative which has been discussed in the literature for several years. While the source-side wavefield for primary imaging relates to a single shot location, the down-going wavefield used in multiple imaging utilises all receivers as secondary sources, thus significantly increasing the illumination from the surface (Berkhout and Verschuur, 1994). The concept was developed further by Whitmore et al. (2010) who used up-going and down-going wavefields from a dual-sensor towed-streamer. One complication arising from multiple imaging is cross-talk, where different orders of surface scattering can contaminate the image. Lu et al. (2016) describe a practical approach to attenuate this noise based on predicting and subtracting causal and anti-causal cross-talk. The use of least-squares migration of multiples has also been documented as a way to attenuate cross-talk (for example, Zhang and Schuster, 2014, or Lu et al., 2018).

We compare results from least-squares multiple imaging using towed-streamer and ocean-bottom-node (OBN) acquisitions from the Central North Sea. We discuss how using least-squares multiple migration constrained jointly by towed-streamer and OBN data may be used to get the best from both acquisitions.

Method

Our approach follows the least-squares wave-equation multiple migration (LS-WEMM) method described by Poole (2019):

$$m(t,x,y) = S(t,x,y)F^{-1}\Phi(f,x,y,z)D_{\Phi}(f,x,y,z)r(x,y,z). \quad (1)$$

In this formulation, the reflectivity, $r(x,y,z)$, is derived such that, when it is convolved with the forward extrapolated down-going wavefield, $D_{\Phi}(f,x,y,z)$, and further extrapolated to the surface using operator $\Phi(f,x,y,z)$, the up-going multiple wavefield, $m(t,x,y)$, is produced to compare with recorded multiples in a least-squares sense. Confidence weights, $S(t,x,y)$, limit the cost function to recorded data locations within the mute. Spatial coordinates are given by (x,y,z), t and f refer to time and temporal frequency, respectively, and the inverse Fourier transform, F^{-1}, converts data from the frequency domain to the time domain. In practice, recorded data are used as a substitute for the recorded multiples. The reflectivity, derived using a steepest descent iterative solver, represents the subsurface to predict the following order of arrivals from the down-going wavefield. For example, primaries will predict first-order multiples, first-order multiples will predict second order-multiples, and so on.

Depending on the complexity of the velocity model, various extrapolation operators may be employed. One-way wave-equation extrapolators include phase-shift-plus-interpolation, finite difference, or Fourier finite difference (Biondi, 2006, provides more information on each of these).

As our examples will show, towed-streamer and OBN data each bring benefits to multiple imaging. As such, we propose least-squares multiple imaging constrained jointly by both towed-streamer and OBN data. Extending the nomenclature of Equation 1, this involves consideration of separate forward extrapolated down-going wavefields ($D_{\Phi,TS}$ and $D_{\Phi,OBN}$), confidence weights (S_{TS} and S_{OBN}), and up-going multiple wavefields (m_{TS} and m_{OBN}) as given in Equation 2, where *TS* and *OBN* refer to towed-streamer and OBN data respectively. The confidence weights may also be used to give one dataset more importance than the other. The approach may be extended to include additional data volumes.

$$\begin{pmatrix} m_{TS}(t,x,y) \\ m_{OBN}(t,x,y) \end{pmatrix} = \begin{pmatrix} S_{TS}(t,x,y) \\ S_{OBN}(t,x,y) \end{pmatrix} F^{-1}\Phi(f,x,y,z) \begin{pmatrix} D_{\Phi,TS}(f,x,y,z) \\ D_{\Phi,OBN}(f,x,y,z) \end{pmatrix} r(x,y,z) \quad (2)$$

Real data examples

The data examples come from a ~250 km^2 area located in the Central North Sea, covered by both towed-streamer and OBN data sets. The vintage towed-streamer data consisted of two acquisitions, deploying 8 cables and 10 cables in 2006 and 2009, respectively. Hydrophone-only streamers of 6 km length with 100 m separation were used, along with conventional dual-source (flip-flop) airgun arrays. The OBN survey included a 50 m × 50 m shot carpet and was acquired in 2020.

The towed-streamer data were pre-processed through swell-noise attenuation, wavefield separation and regularisation. Figure 1a shows a depth slice at 140 m from one sail-line after demultiple, imaged with common-shot wave-equation migration (WEM), and Figure 1b shows the corresponding depth slice for LS-WEMM using the data before demultiple. The inset zoom highlights the increased image coverage of LS-WEMM compared to common-shot primary-WEM (as illustrated by the yellow arrows).

The OBN data were pre-processed through PZ calibration, shot-point regularisation, up-down separation and source designature. Figure 1c shows a mirror-WEM of the down-going data for one receiver line after demultiple, and Figure 1d shows LS-WEMM of down-going data for the same receiver line. Common-receiver domain LS-WEMM was used for these tests, thus imaging the source-side multiples. The down-going mirror-WEM image coverage (Figure 1c) from one receiver-line is similar to that of one towed-streamer sail-line (Figure 1a). The corresponding LS-WEMM for one receiver line (Figure 1d), however, shows much larger image coverage than for one towed-streamer (Figure 1b), providing imaging coverage over the full 6 km offset range (in x and y) input to this test.

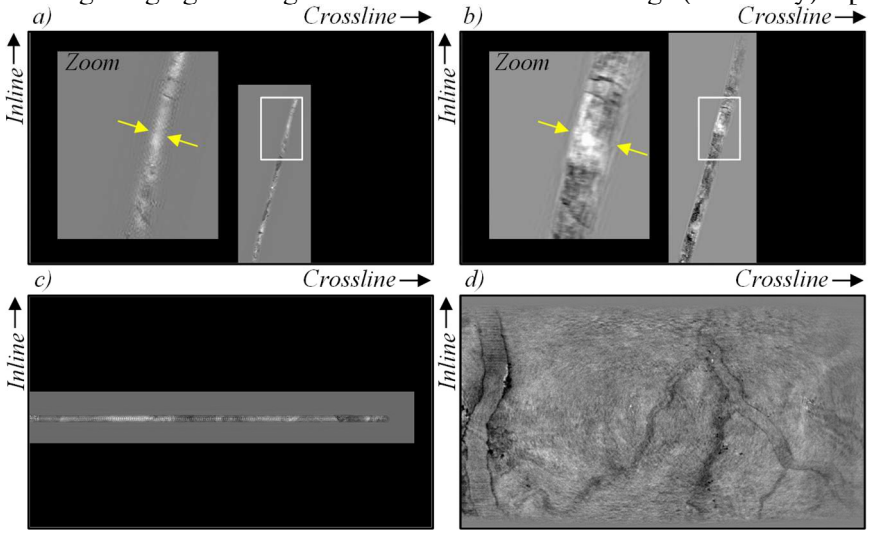

Figure 1 *Imaged depth slice at 140 m from a single acquisition line. Towed-streamer: a) common-shot primary-WEM, b) LS-WEMM. OBN: c) down-going mirror-WEM, d) down-going LS-WEMM.*

Figure 2 compares imaging results for the area using all acquisition lines. Figure 2a shows a depth slice at 170 m from the towed-streamer common-shot primary-WEM. The depth slice exhibits acquisition striping parallel to the sail-line direction (as annotated in Figure 2a) due to the lack of near-offset data recorded by the outer streamers. This is further illustrated by the vertical section (Figure 2b) which is approximately perpendicular to the sail-line direction and exhibits holes in coverage and limited vertical resolution in the shallow. Figures 2c and 2d show corresponding LS-WEMM results, exhibiting improved vertical resolution in the shallow and reduced acquisition striping. This is due to the richer illumination and smaller reflection angles offered by the multiple energy.

Figures 2e and 2f show a depth slice and a vertical section perpendicular to the receiver-line direction (as annotated in Figure 2e), respectively, from a down-going OBN mirror-WEM. Although down-going mirror migrations are well known to reduce acquisition striping, in this example the problem was not fully mitigated in the shallow. The OBN down-going LS-WEMM results, given in Figures 2g and 2h, exhibit reduced acquisition striping and increased image coverage, due to the rich illumination offered by multiple imaging. Some slight residual shot-point acquisition footprint can be seen on the image, which is discussed later with reference to Figure 3. The arrows highlight improved illumination of some channels on the OBN LS-WEMM result compared to towed-streamer LS-WEMM.

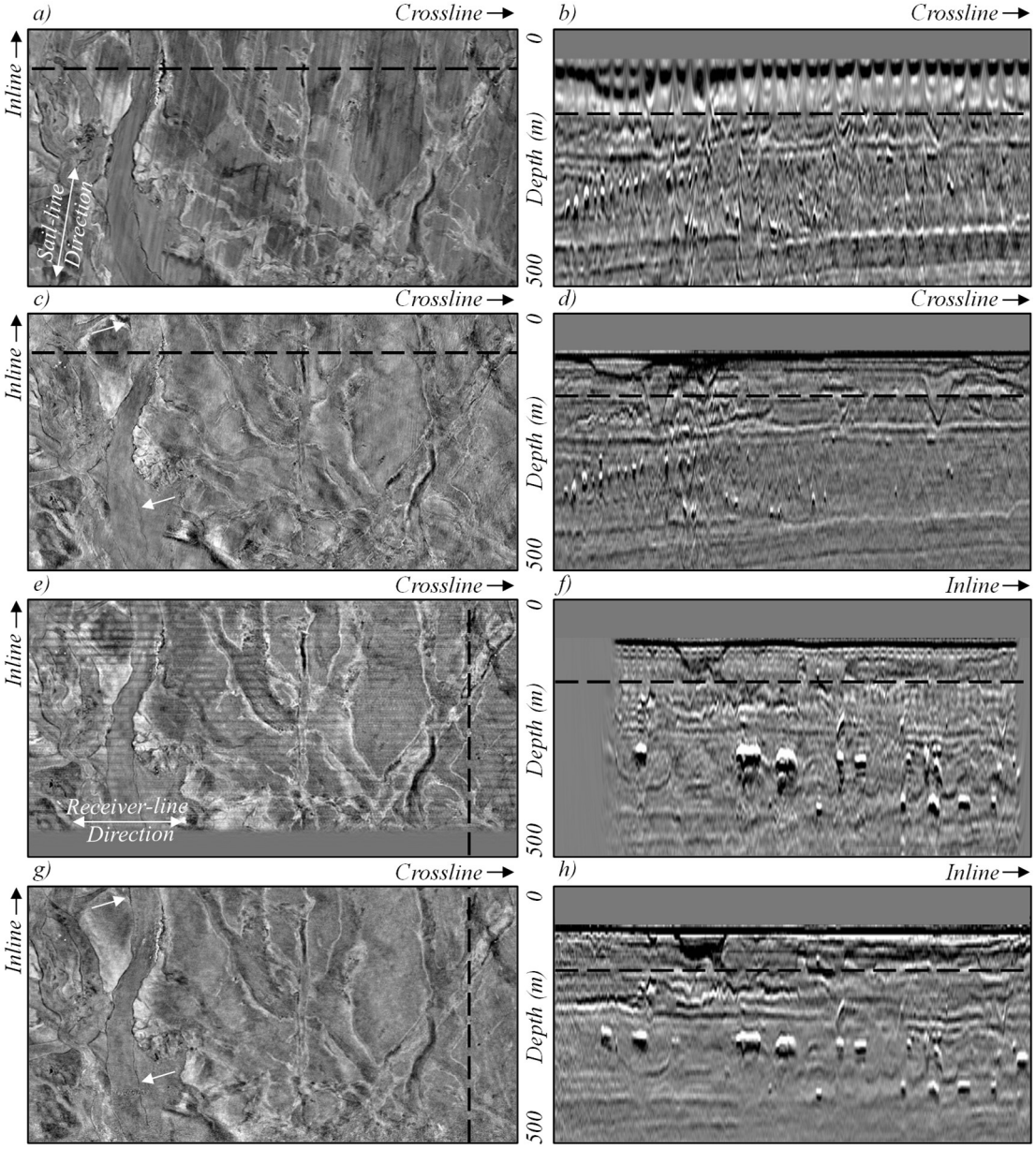

Figure 2 *Imaging using all acquisition lines. Towed streamer: a) & b) common-shot primary-WEM, c) & d) LS-WEMM. OBN: e) & f) down-going demultiple WEM, g) & h) down-going LS-WEMM. Left column: depth slices at 170 m. Right column: vertical sections as annotated with the dashed lines.*

Figures 3a and 3b show LS-WEMM results for towed-streamer and OBN data, respectively. The OBN result provides more consistent illumination overall; for example, better contrast of the channel features and reduced cross-talk (see arrows). This is due to the diverse illumination and considerable overlap between receiver lines offered by the OBN acquisition. In contrast, we observe better resolution for the towed-streamer results. In part, this is due to the OBN offset distribution being more heavily weighted towards longer offsets, which suffer more from attenuation. In addition, OBN data is inherently richer in low frequencies due to the lack of a short-period receiver ghost. Finally, as illumination for multiple imaging occurs at all offsets, shot-to-shot feather variations in the towed-streamer case lead to enriched sampling and better lateral resolution compared to the nominal zero-feather case. The OBN acquisition does not benefit from this effect as all receiver gathers share the same shot positions, leading to a residual shot-point footprint in the OBN result (highlighted by the white rectangle).

Results from LS-WEMM using an OBN/towed-streamer joint cost function are given in Figure 3c. We can see how this result has retained the benefits of the improved OBN image consistency, with almost all of the resolution of the towed-streamer image. This provides a convenient way to capitalise on the combined spatial sampling of both towed-streamer and OBN datasets.

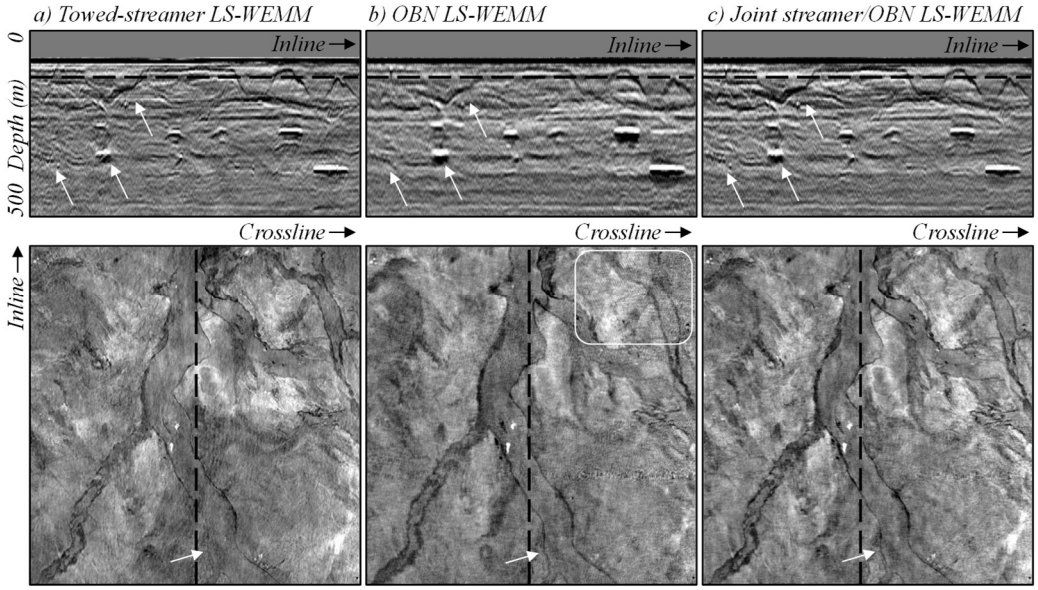

Figure 3 *Imaging comparisons for: a) towed-streamer LS-WEMM, b) OBN LS-WEMM, and c) joint towed-streamer/OBN LS-WEMM. Top: crossline vertical section, bottom: depth slice at 140 m.*

Conclusions

We have compared imaging results using towed-streamer and OBN data from the Central North Sea. In comparison to primary imaging, LS-WEMM using either data type reduced acquisition striping and improved spatial resolution. Focussing on LS-WEMM, towed-streamer data were shown to offer better lateral resolution, whereas OBN data provide more spatial consistency in the image, due to the extra illumination of the OBN geometry. We proposed a LS-WEMM method constrained jointly by towed-streamer and OBN data, which combined the benefits of both data sets.

Acknowledgements

We would like to thank CGG Multi-Client & New Ventures for permission to show the data examples.

References

Berkhout, A.J and Verschuur, D.J. [1994] Multiple technology: Part 2, migration of multiple reflections. *64th Annual International Meeting*, SEG, Expanded Abstracts, 1497-1500.

Biondi, B.L. [2006] 3D seismic imaging. *Investigations in Geophysics*, SEG publication.

Davies, D. and Tillotson, P. [2019] Near field hydrophones – Imaging the subsurface. *81st EAGE Conference and Exhibition*, Extended Abstracts, We R4 9.

Dhelie, P.E., Danielsen, V., Lie, J.E., Støen, S., Dustira, A., Ackers, M.A., Schjelderup, S., Dancer, K., Ramsay, M. and Larssen, B. [2020] 3D seismic in the Barents Sea using quadro point sources for zero-offsets and accurate AVO analysis. *82nd EAGE Conference and Exhibition*, Extended Abstracts, We Dome3 4.

Lu, S., Whitmore, D., Valenciano, A., Chemingui, N. and Ronholt, G. [2016] A practical crosstalk attenuation method for separated wavefield imaging. *86th Annual International Meeting,* SEG, Expanded Abstracts, 4235-4239.

Lu, S., Liu, F., Chemingui, N., Valenciano, A. and Long, A. [2018] Least-squares full-wavefield migration. *The Leading Edge*, **37**(1), 46-51.

Poole, G. [2019] Shallow water surface related multiple attenuation using multi-sailline 3D deconvolution imaging. *81st EAGE Conference and Exhibition*, Extended Abstracts, Tu R1 5.

Vinje, V., Lie, J.E., Danielsen, V., Dhelie, P.E., Siliqi, R., Nilsen, C-I., Hicks, E. and Camerer, A. [2017] Shooting over the streamer spread. *First Break*, **35**, 97-104.

Whitmore, N.D., Valenciano, A.A., Sollner, W. and Lu, S. [2010] Imaging of primaries and multiples using a dual-sensor towed streamer. *80th Annual International Meeting,* SEG, Expanded Abstracts, 3187-3192.

Zhang, D. and Schuster, G.T. [2014] Least-squares reverse time migration of multiples. *Geophysics*, **79**, S11–S21.